A small increase in *CHEK1* activity leads to the arrest of the first zygotic division in human

Beili Chen[1,5,#], Jianying Guo[2,6#], Ting Wang[2,6#], Qianhui Lee[4], Jia Ming[2], Fangfang Ding[1,5], Haitao Li[2,6], Zhiguo Zhang[1,5,*], Lin Li[4,*], Yunxia Cao[1,5,*] and Jie Na[2,*]

[1]Reproductive Medicine Center, Department of Obstetrics and Gynecology, the First Affiliated Hospital of Anhui Medical University, Anhui, China

[2]School of Medicine, Tsinghua University, Beijing, 100084, China

[3]Department of Chemistry, Tsinghua University, Beijing, 100084, China

[4]Central Laboratory, Beijing Obstetrics and Gynecology Hospital, Capital Medical University, Beijing, 100026, China

[5]NHC Key Laboratory of study on abnormal gametes and reproductive tract (Anhui Medical University), Anhui, China

[6]Tsinghua-Peking Center for Life Sciences, Beijing, 100084, China

[#]Equal contribution.

[*]**Correspondence:** Jie Na (Ph.D.), e-mail: jie.na@tsinghua.edu.cn

Yunxia Cao (Ph.D.), e-mail: caoyunxia6@126.com

Lin Li (Ph.D.), e-mail: linlithu@ccmu.edu.cn

Zhiguo Zhang (Ph.D.), e-mail: zzg_100@163.com

Running title: *CHEK1* mutation leads to the arrest of the first zygotic division in human

Keywords: zygote, mitosis, CHEK1, DNA damage checkpoint, assisted reproduction

The first mitotic division in mammalian zygotes is unique. The fertilized egg reactivates its cell cycle, and the maternal and paternal genomes start to reprogram to become totipotent. The first division is very sensitive to a range of perturbations, particularly the DNA damage, leading to the embryo's failure to enter the first mitosis. We discovered that a point mutation in the human *CHEK1* gene resulted in an Arginine 442 to Glutamine change at the C-terminus of the CHEK1 protein. *CHEK1* R442Q mutation caused the zygote to arrest just before the first division. Heterozygote individuals appeared to be healthy except that the female carriers are infertile. Expressing the corresponding mouse mutant Chk1 protein in zygotes also caused arrest before the first mitosis. Treating Chk1

R442Q mouse zygotes with low concentrations of CHEK1 inhibitor enabled the embryos to overcome the cell cycle arrest and resume normal development. Our results revealed an unexpected zygote mitotic checkpoint, which is extremely sensitive to the CHEK1 kinase activity. The fine-tuning of the DNA damage checkpoint permits the arrested one-cell embryos to overcome the first mitotic block and develop into healthy animals. These findings have important implications in assisted human reproduction.

During the first cell cycle, the mammalian zygotes switch from meiosis to mitosis, both paternal and maternal genomes replicate, and the minor genome activation occurs. In the meantime, the male and female pronucleus move to the center of the zygote and merge. Then zygotes enter the metaphase, and sister chromatids separate into two daughter cells (Clift and Schuh, 2013). Significant epigenetic reprogramming also takes place during this sensitive time window. Thus, many perturbances may cause the first mitosis to fail.

We discovered a family that the female adults were infertile. One female patient underwent in vitro fertilization treatment. Interestingly, 8 out of 15 eggs were fertilized normally as the zygotes contained one female and one male pronucleus, but they all failed to divide into 2-cell embryos (Table 1). Further investigation found that three sisters of this female patient were infertile, while another two sisters had children. With the patients' consent, whole-exome sequencing was carried out in all of the infertile subjects. After the pedigree analysis, we found that a heterozygous missense variant in the *CHEK1* gene, c.1325G>A; p.R442Q, was shared by all the infertile sisters (Figure 1A). The variant was confirmed by Sanger sequencing in the whole family members (Figure 1B). The results suggested that each infertile subject inherited the variant from their father II-8, and the variant was segregated within the whole family (Figure 1A and 1B). CHEK1 protein plays an essential role in the DNA damage response (Chen et al., 2012; Ju et al., 2020; Liu et al., 2000) and is conserved across species (Supplementary Figure 1A). Interestingly, although the same *CHEK1* R442Q variant is expressed in somatic cells, based on RT-PCR and Sanger sequencing analysis of the peripheral blood samples from III-2,3,4,5,6 and 7 (Figure 1C and Supplementary Figure 1B-D), the heterozygote carriers are all healthy. We also analyzed the transcriptome profile of human oocytes, 1 and 2-cell embryos, *CHEK1* transcripts are present at high levels in GV and metaphase II oocytes, zygotes, and 2-cell embryos (Figure 1D). Therefore, it should exist as a maternal protein. Thus, we highly suspect that the *CHEK1* R442Q mutation caused the first zygotic mitosis to arrest.

69 **Table1. Oocyte and embryo phenotypes of IVF attempt for the *CHEK1* R442Q female patients.**

Table 1. Oocyte and Embryo Characteristics of IVF and ICSI Attempts for the Affected Individual

Individual	Age (years)	Duration of Infertility (Years)	IVF and ICSI Attempts	Retrieved Oocytes	MII Oocytes	0PN Oocytes	2PN Oocytes	Cleaved Fertilized Oocytes
III-7	29	2	First IVF	17	15	7	8	0

70

71

72 To test this hypothesis, we cloned mouse Chk1, whose amino acid sequence is 93.07% identical
73 to that of the human CHEK1, and generated the same Chk1 R442Q mutation as found in the
74 infertile patient. Upon overexpression of WT or R442Q Chk1 protein in mouse zygotes by
75 mRNA injection, we found that more than 60% of the Chk1 R442Q zygotes failed to divide
76 into 2-cell embryos (Figure 2A and B). Overexpression of Chk1 WT did not affect the first
77 mitosis (Figure 2B and C). It has been shown that overexpression of Chk1 in mouse GV
78 oocytes caused meiosis I arrest (Chen et al., 2012). Interestingly, when we overexpressed Chk1
79 WT and R442Q in GV oocytes, the R442Q caused significantly more oocytes to arrest in
80 metaphase I than WT (Figure 2D-F). We analyzed Chk1 protein localization based on the
81 immunofluorescence signal, both Chk1 WT and R442Q proteins localized in the nucleus and
82 on the spindle during mitosis and meiosis (Supplementary Figure 2A and C). The amount of
83 overexpressed mutant protein is less than the overexpressed WT protein (Supplementary
84 Figure 2B and D), based on their respective mean fluorescence intensity (MFI), suggesting that
85 the R442Q change did not stabilize Chk1 protein.

86

87 As the activation of CHEK1 kinase in response to DNA damage will cause cell cycle arrest in
88 the G2 phase (Patil et al., 2013), we hypothesize that the R442Q mutation may cause an
89 increase in CHEK1 protein kinase activity. Therefore, we generated the N-terminus kinase
90 domain, the full-length, and the full-length R442Q mutant CHEK1 proteins and performed the
91 kinase assay. Indeed, the N-terminus kinase domain had very high kinase activity, as reported
92 by several studies (Caparelli and O'Connell, 2013; Emptage et al., 2017; Goto et al., 2015; Han
93 et al., 2016; Tapia-Alveal et al., 2009; Walker et al., 2009). The R442Q mutant protein had
94 about twice as high kinase activity as the WT protein (Figure 3A, Supplementary Figure 3).
95 We next ask whether Chk1 R442Q may induce more DNA damage in zygotes. Interestingly,
96 overexpression of Chk1 R442Q reduced γH2AX staining in the male pronucleus (Figure 3B
97 and C, Supplementary Figure 4A). Since R442Q mutant protein has higher kinase activity than

98 the WT protein, we used a CHEK1 inhibitor CCT244747 to treat zygotes overexpressing WT
99 or R442Q. As expected, CCT244747 rescued the first mitosis arrest caused by R442Q, nearly
100 all treated R442Q zygotes divided into 2-cell embryos (Supplementary Figure 4B). However,
101 regular CCT244747 dosage also increased DNA damage, as shown by stronger γH2AX
102 staining in treated WT or R442Q embryos (Supplementary Figure 4C and D). Since R442Q
103 mutant has approximately double kinase activity than WT protein, we reasoned that reducing
104 the kinase activity close to the normal level might be sufficient to overcome the first mitotic
105 arrest. Indeed, 30 nM of CCT244747 permitted R442Q zygotes to divide into 2-cell embryos
106 and did not increase the γH2AX signal (Figure 3D-G, Supplementary Figure 4D-F). Moreover,
107 60% of 30 nM CCT244747 treated R442Q zygotes developed to the blastocyst stage (Figure
108 3H and I). We examined the expression of pluripotency genes and found that Oct4 and Nanog
109 proteins are highly expressed in the inner cell mass of CCT244747 treated R442Q blastocysts
110 (Figure 3J). Treated WT and R442Q blastocysts also had a similar number of total cells and
111 Oct4 and Nanog positive cells (Figure 3K), suggesting that their development was not
112 compromised.
113
114 We next performed transcriptome profiling of zygotes, 2-cell embryos, and blastocysts injected
115 with mRNA encoding WT or R442Q with or without low dosage CHEK1 inhibitor treatment
116 (Figure 4A). Principal component analysis (PCA) and heatmap clustering showed that 1-cell
117 arrested R442Q zygotes clustered together with PN5 WT zygotes (Figure 4B and C),
118 suggesting that the minor zygotic genome activation was not affected. At the late 2-cell stage,
119 the transcriptome of R442Q embryos, which managed to divide, clustered together with WT
120 2-cell embryos (Figure 4B and C), indicating that the major zygotic genome activation occurred
121 in these embryos. The CHEK1 inhibitor rescued WT and R442Q blastocysts clustered together,
122 consistent with our previous observations (Figure 4B and C, Figure 3J and K). We analyzed
123 differentially expressed transcripts in WT and R442Q zygotes and 2-cell embryos. Compare to
124 WT embryos, R442Q zygotes downregulated RNA processing and cell division related genes.
125 R442Q 2-cell embryos decreased the expression of some RNA processing and chromatin
126 modification genes but increased genes associated with nucleotide metabolism (Supplementary
127 Figure 5). Finally, we transferred CHEK1 inhibitor rescued R442Q 2-cell embryos into female
128 mice and found that a similar number of pups were born compared with the WT embryo
129 transferred group (Figure 4D and E, Supplementary Figure 3G). These results suggest that the
130 low concentration of CHEK1 inhibitor treatment may relieve zygotes from the first mitotic

131 division arrest caused by a slight tightening up of DNA damage checkpoint, and the rescued
132 embryos would develop normally.
133
134 The discovery of the *CHEK1* R442Q mutation and the first zygotic mitosis arrest phenotype in
135 human reproduction has important implications. All the heterozygous female carriers are
136 infertile, presumably due to failed mitosis in zygotes. As the zygotes contained mostly maternal
137 proteins inherited from the egg, both CHEK1 WT and R442Q proteins should be present in the
138 carrier's eggs. Based on the clinical observation during the IVF treatment, CHEK1 R442Q did
139 not affect oocyte meiosis, suggesting that a small elevation in CHEK1 kinase activity does not
140 block the first meiotic division in women. The II-8 and III-8 male carriers are healthy and do
141 not have fertility problems, indicating that *CHEK1* R442Q does not affect sperm meiosis in
142 men. CHEK1 is a ubiquitously expressed protein, and all the heterozygous individuals are
143 healthy without cancer or autoimmune diseases based on a consent health history survey. Thus,
144 CHEK1 R442Q should not affect most mitotic division of embryonic or adult cells. All the
145 heterozygous females inherited the *CHEK1* R442Q mutation from their father as their mother
146 has two copies of the normal *CHEK1* gene. Since the paternal genome starts to express after
147 the major zygotic genome activation during the 4 to 8-cell stage in humans (Kermi et al., 2019;
148 Khokhlova et al., 2020; Xue et al., 2013; Yan et al., 2013), the CHEK1 R442Q protein derived
149 from the mutated paternal copy of *CHEK1* will likely be present from the 8-cell stage onwards.
150 Therefore, the small elevation of CHEK1 kinase activity does not appear to arrest cell division
151 after the 8-cell stage in human embryos. Thus, the CHEK1 R442Q protein seemed to affect the
152 first mitotic division most seriously, indicating that the first mitosis is particularly sensitive to
153 DNA damage checkpoint activation in humans. Moreover, the DNA damage checkpoint
154 threshold may be cell type, developmental stage, and species-dependent, based on the human
155 phenotype and our results obtained in the mouse system. When we treat Chk1 R442Q
156 overexpressing mouse zygotes with a low dosage of CHEK1 inhibitor, they can escape the first
157 mitotic arrest and develop normally. CHEK1 inhibitors are often used as cancer drugs. They
158 inhibit the DNA damage checkpoint, making cancer cells accumulate DNA damage and die
159 (Dent et al., 2011; Goto et al., 2012; McNeely et al., 2014; Smith et al., 2010; Zhang and Hunter,
160 2014). Surprisingly, although a high dosage of CHEK1 inhibitor also induced DNA damage in
161 zygotes, a low dosage of CHEK1 inhibitor rescued R442Q overexpression induced first mitosis
162 arrest without eliciting any DNA damage judging by the γH2AX staining, and the embryos
163 developed normally. Chk1 R442Q overexpression also did not induce γH2AX signal. The

above results suggested that small up or down-regulation of CHK1 kinase activity may not affect genome stability. Our findings also imply the possibility to use low dosage CHEK1 inhibitor treatment to release cells from low-level genome stress induced cell cycle block during zygote mitosis or other sensitive periods.

METHODS

Patient consent and ethical approvement

The proband III-7 and her family were recruited for this study from the First Affiliated Hospital of Anhui Medical University. The human sample collection and analysis was approved by the Ethics Committee for Clinical Medical Research of the First Affiliated Hospital of Anhui Medical University and carried out with informed consent.

Whole-exome sequencing (WES) analysis

Libraries were generated using the Agilent SureSelect Human All Exon V6 kit (Agilent Technologies, USA) following the manufacturer's recommendations. WES was carried out on an Illumina NovaSeq6000 sequencer with pair end 150 bp (PE150) for each reaction. The original sequencing reads were aligned to the reference genome GRCh37/hg19, variants including single nucleotide polymorphisms (SNPs) and short insertion and deletion (INDELs) were called using the GATK software program. The identified variants were further annotated using ANNOVAR software. The criteria used for filtering the desired variants were as follows (i) missense, nonsense, frameshift, or splice site variants; (ii) variants with minor allele frequency < 1%. The minor allele frequency data were obtained by referring to the following databases: Genome Aggregation Database (gnomAD, http://gnomad.broadinstitute.org/), 1000 Genomes (1000G, http://browser.1000genomes.org/index.html), and the NHLBI Exome Sequencing Project (ESP6500).

Quantitative PCR

Total RNA of patient and control blood samples were extracted with TRIZOL (Invitrogen). 1μg RNA of each sample was used for reverse transcription with Superscript II (Invitrogen). Q-PCR reactions were performed using GoTaq qPCR Master Mix (Promega) in a CFX96 Real-Time System (Bio-Rad). The relative expression level of each gene was normalized against the Ct (Critical Threshold) value of the house-keeping gene GAPDH using the Bio-Rad CFX Manager program. For detecting the mutation transcript in the patient's somatic cells, qPCR

197 products were purified by agarose gel electrophoresis, ligated to pEASY-T5 Zero plasmid
198 (TransGen CT501-01), and sequenced using the M13 forward primer. QPCR primer used in
199 this study:
200 *hCHEK1*-F: CAACAACTGATAGGAGAAACAATAAACT;
201 *hCHEK1*-R: CAAATCTTCTGGCTGCTCACAATA;
202 *hGAPDH*-F: TGATGACATCAAGAAGGTGGTGAAG;
203 *hGAPDH*-R: TCCTTGGAGGCCATGTGGGCCAT.
204
205 **Mouse embryo culture and microinjection**
206 All animal experiments were conducted following the Guide for the Care and Use of Animals
207 for Research Purposes. The protocol for mouse embryo isolation was approved by the
208 Institutional Animal Care and Use Committee and Internal Review Board of Tsinghua
209 University. Embryos were collected from wild type C57BL/6 females (Charles River). Zygotes
210 for RNA injection were collected from mated female mice 26-28 hrs post-HCG, then cultured
211 in KSOM medium (Merck Millipore MR-106-D) in 37.5℃ 5% CO_2 incubator. GV oocytes
212 were collected from the ovary of C57BL/6 female in M2 medium (Sigma M7167)
213 supplemented with 10μM Cilostamide (Cayman 14455). Microinjection of mRNAs at a
214 concentration of 200 ng/μl into the mouse GV oocytes or PN3 zygotes was performed on a
215 Leica microscope micromanipulator. The microinjected embryos were treated with or without
216 CHEK1 inhibitor CCT244747 (MedChemExpress, HY-18175/CS-5919) at different
217 concentrations as indicated.
218
219 **Plasmid cloning and RNA synthesis**
220 Mouse *Chk1* cDNA was cloned into the RN3P vector for in vitro transcription of mRNA.
221 mRNAs were generated using the T3 mMESSAGE mMACHINE Kit according to the
222 manufactures instructions (Ambion).
223
224 **CHEK1 protein production and kinase assay**
225 For human CHEK1 protein purification and kinase assay, N-term (1-289aa), WT full length,
226 and mutant full-length human *CHEK1* cDNAs were cloned from 293FT cells, fused with 6×His
227 tag at the N-terminus, and cloned into Bac-to-Bac Baculovirus Expression System following
228 the instructions of the manufactures (Invitrogen 10359-016).

229 For kinase assay, Sf9 insect cells cultured in suspension in ESF 921 Insect Cell Culture
230 Medium (Expression, 96-001) were used for protein overexpression and purification.
231 Baculovirus of His-tagged N-term (1-289aa), WT full length, and mutant full-length human
232 *CHEK1* were introduced into the sf9 insect cells by Cellfectin II Reagent (Thermo, 10362100)
233 following the instructions of the manufactures. Recombinant Proteins were purified with
234 affinity Ni-NTA agarose from approximately $2x10^8$ infected cells. Purified proteins were
235 verified by Coomassie bright blue stain and Western blot with the antibody of CHEK1 and
236 His-tag. The secondary antibodies used were HRP-conjugated Goat Anti-Rabbit (Jackson
237 ImmunoResearch, 111-065-003), HRP-conjugated Goat Anti-Mouse
238 (Jackson ImmunoResearch, 111-035-003). CHEK1 kinase assay was conducted using the
239 kinase assay kit (Beyotime, S0150) with the substrate of Cdc25C-derived Chktide (Sigma-
240 Aldrich, 12-373).
241
242 **Immunostaining and confocal microscopy**
243 For immunostaining, mouse oocytes or embryos were fixed in 1% PFA overnight, then
244 permeabilized with 0.25% Triton X-100 for 20 min. Embryos were then blocked with 5% FCS
245 at room temperature for 2 h and incubated with primary antibody overnight at 4℃, followed
246 by washing in PBST and incubating with secondary antibody for 1 h at room temperature.
247 Antibodies used in this study are: CHEK1 (Abcam, ab32531), Oct4 (Abcam, ab19857), gamma
248 H2A.X (phospho S139, Abcam, ab26350), Tubulin (Abcam, ab6160), Nanog (CST, 4903P).
249 Secondary antibodies used are: Dylight 488-conjugated Goat Anti-Mouse (Thermo, 35502),
250 Dylight 488-Goat Anti-Rabbit (Thermo, A32727), Dylight 549-conjugated Goat Anti-Mouse
251 (Thermo, 35552), and Dylight 549-conjugated Goat Anti-Rabbit (Thermo, 35557). DNA was
252 stained by DAPI (Sigma-Aldrich, 28718-90-3). Immunostaining images were acquired with a
253 Nikon A1 confocal microscope using an oil-immersion 40× objective. Raw data were
254 processed using open-source image analysis software Fiji ImageJ.
255
256 **Transcriptome Profiling**
257 For gene expression study in mouse preimplantation embryos, we used the SMART-seq2
258 protocol to amplify single embryo RNA (Picelli et al., 2014). Embryos were first lysed in
259 hypotonic lysis buffer (Amresco, M334), followed by reverse transcription and pre-
260 amplification. After AMPure XP beads purification, the cDNA libraries were tagmented by

261 Tn5 and were subject to Illumina Nextera library preparation. All libraries were sequenced on
262 Illumina HiSeq X-10 according to the manufacturer's instruction.
263
264 **RNA-seq data processing**
265 Adapter sequences were trimmed using TrimGalore (version 0.4.4). Clean reads were mapped
266 to the mouse genome (mm10) using Bowtie2 (version 2.3.5) software with the Refseq
267 annotation. Gene expression values were represented with FPKM (Fragments Per Kilobase per
268 Million) calculated by RSEM (version 1.2.28). Differential expression genes (DEGs) were
269 analyzed using the DESeq2 package (version 1.20.0). Genes that satisfied the threshold "fold
270 change $\geqslant 2$, $p < 0.01$" were considered significant DEGs. Principle component analyses were
271 performed using R's "prcomp" function and drawn by ggplot2 package (version 3.1.0). The
272 heatmaps were produced by the heatmap2 function of the gplots package (version3.0.1.1) with
273 the hierarchical clustering method. The enrichment of GO was analyzed using clusterProfiler
274 package (version 3.8.1).
275
276 **Statistical analysis**
277 Data are presented as mean ± standard error of the mean (SEM). Statistical significance was
278 determined by Student's t-test (two-tail) for two groups; one-way or two-way Analysis of
279 Variance (ANOVA) for multiple groups using Graphpad software. $P < 0.05$ was considered
280 significant.
281
282 **ACKNOWLEDGEMENTS**
283 This work was supported by the National Key R&D Program of China Grant
284 2019YFA0110001, 2017YFA0102802; the National Natural Science Foundation of China
285 (NSFC) Grant 31970819, 91740115, 31771108 to JN. NSFC Grant 32000610 to JG, 82001516
286 to BC, and 82071724 to ZZ. JG is supported by the Tsinghua-Peking Center for Life Sciences
287 postdoctoral fellowship.
288
289 **AUTHOR CONTRIBUTIONS**
290 BC, JG, TW, QL, ZZ, LL, YC, and JN conceived the study and designed the experiments. JG,
291 TW, QL, JM performed mouse embryo and oocytes collection and microinjection, phenotype
292 analysis, and transcriptome profiling; BC and FD performed clinical sample collection and data

analysis, HL instructed protein kinase activity study, JG, BC, TW, ZZ, LL, YC and JN wrote the manuscript. All authors read and approved the final version of the manuscript.

COMPETING INTEREST STATEMENT

The authors declare no competing interests.

Data availability

Raw and processed RNA-seq data are available at the Gene Expression Omnibus GEO by accession number GSE163765. All other relevant data are available from the corresponding author upon request.

References

Caparelli, M.L., and O'Connell, M.J. (2013). Regulatory motifs in Chk1. Cell Cycle *12*, 916-922.

Chen, L., Chao, S.B., Wang, Z.B., Qi, S.T., Zhu, X.L., Yang, S.W., Yang, C.R., Zhang, Q.H., Ouyang, Y.C., Hou, Y.*, et al.* (2012). Checkpoint kinase 1 is essential for meiotic cell cycle regulation in mouse oocytes. Cell Cycle *11*, 1948-1955.

Clift, D., and Schuh, M. (2013). Restarting life: fertilization and the transition from meiosis to mitosis. Nature Reviews Molecular Cell Biology *14*, 549-562.

Dent, P., Tang, Y., Yacoub, A., Dai, Y., Fisher, P.B., and Grant, S. (2011). CHK1 Inhibitors in Combination Chemotherapy Thinking Beyond the Cell Cycle. Mol Interv *11*, 133-140.

Emptage, R.P., Schoenberger, M.J., Ferguson, K.M., and Marmorstein, R. (2017). Intramolecular autoinhibition of checkpoint kinase 1 is mediated by conserved basic motifs of the C-terminal kinase-associated 1 domain. Journal of Biological Chemistry *292*, 19024-19033.

Goto, H., Izawa, I., Li, P., and Inagaki, M. (2012). Novel regulation of checkpoint kinase 1: Is checkpoint kinase 1 a good candidate for anti-cancer therapy? Cancer Sci *103*, 1195-1200.

Goto, H., Kasahara, K., and Inagaki, M. (2015). Novel Insights into Chk1 Regulation by Phosphorylation. Cell Struct Funct *40*, 43-50.

Han, X.Z., Tang, J.S., Wang, J.N., Ren, F., Zheng, J.H., Gragg, M., Kiser, P., Park, P.S.H., Palczewski, K., Yao, X.S.*, et al.* (2016). Conformational Change of Human Checkpoint Kinase 1 (Chk1) Induced by DNA Damage. Journal of Biological Chemistry *291*, 12951-12959.

Ju, J.Q., Li, X.H., Pan, M.H., Xu, Y., Sun, M.H., Xu, Y., and Sun, S.C. (2020). CHK1 monitors spindle assembly checkpoint and DNA damage repair during the first cleavage of mouse early embryos. Cell Proliferat *53*.

Kermi, C., Aze, A., and Maiorano, D. (2019). Preserving Genome Integrity during the Early Embryonic DNA Replication Cycles. Genes-Basel *10*.

Khokhlova, E.V., Fesenko, Z.S., Sopova, J.V., and Leonova, E.I. (2020). Features of DNA Repair in the Early Stages of Mammalian Embryonic Development. Genes-Basel *11*.

331 Liu, Q.H., Guntuku, S., Cui, X.S., Matsuoka, S., Cortez, D., Tamai, K., Luo, G.B., Carattini-
332 Rivera, S., DeMayo, F., Bradley, A., *et al.* (2000). Chk1 is an essential kinase that is regulated
333 by Atr and required for the G(2)/M DNA damage checkpoint. Gene Dev *14*, 1448-1459.
334 McNeely, S., Beckmann, R., and Lin, A.K.B. (2014). CHEK again: Revisiting the development
335 of CHK1 inhibitors for cancer therapy. Pharmacol Therapeut *142*, 1-10.
336 Patil, M., Pabla, N., and Dong, Z. (2013). Checkpoint kinase 1 in DNA damage response and
337 cell cycle regulation. Cellular and Molecular Life Sciences *70*, 4009-4021.
338 Picelli, S., Faridani, O.R., Bjorklund, A.K., Winberg, G., Sagasser, S., and Sandberg, R. (2014).
339 Full-length RNA-seq from single cells using Smart-seq2. Nat Protoc *9*, 171-181.
340 Smith, J., Tho, L.M., Xu, N.H., and Gillespie, D.A. (2010). The ATM-Chk2 and ATR-Chk1
341 Pathways in DNA Damage Signaling and Cancer. Adv Cancer Res *108*, 73-112.
342 Tapia-Alveal, C., Calonge, T.M., and O'Connell, M.J. (2009). Regulation of Chk1. Cell Div *4*.
343 Walker, M., Black, E.J., Oehler, V., Gillespie, D.A., and Scott, M.T. (2009). Chk1 C-terminal
344 regulatory phosphorylation mediates checkpoint activation by de-repression of Chk1 catalytic
345 activity. Oncogene *28*, 2314-2323.
346 Xue, L., Cai, J.Y., Ma, J., Huang, Z., Guo, M.X., Fu, L.Z., Shi, Y.B., and Li, W.X. (2013).
347 Global expression profiling reveals genetic programs underlying the developmental divergence
348 between mouse and human embryogenesis. Bmc Genomics *14*.
349 Yan, L.Y., Yang, M.Y., Guo, H.S., Yang, L., Wu, J., Li, R., Liu, P., Lian, Y., Zheng, X.Y.,
350 Yan, J., *et al.* (2013). Single-cell RNA-Seq profiling of human preimplantation embryos and
351 embryonic stem cells. Nat Struct Mol Biol *20*, 1131-+.
352 Zhang, Y.W., and Hunter, T. (2014). Roles of Chk1 in cell biology and cancer therapy. Int J
353 Cancer *134*, 1013-1023.
354
355

356 **Figure legends**

357 **Figure 1. First mitosis failure in zygotes from *CHEK1* R442Q females**

358 (A) Genetic analysis in the families carrying *CHEK1* R442Q. Black circles indicate the affected
359 individuals, and the circles with slashes indicate the suspected individuals (III-4 and III-7 had
360 been confirmed during IVF cycles, III-3 and III-6 females were infertile, possibly caused by
361 the arrest of the embryo cleavage). The black arrowhead indicates the proband.

362 (B) Sanger sequencing result of *CHEK1* R442Q mutation in Affected, Infertile, and Carrier
363 individuals. Double peak at the 1325 position highlights the mutated nucleotide.

364 (C) QPCR result confirmed that *CHEK1* R442Q transcripts are present in patients' somatic
365 cells. Left panel, the expression levels of CHEK1 mRNA in human blood cells. Right panel,
366 the ratio of *CHEK1* R442Q mutant transcript in patient somatic cells verified by Sanger
367 sequencing.

368 (D) *CHEK1* expression levels in human and mouse GV oocyte to 2-cell embryo based on RNA-
369 Sequencing data from GSE101571, GSE36552, and GSE71434.

370

371 **Figure 2. Overexpression of *Chk1* R442Q inhibited the first mitosis in mouse zygotes and**
372 **meiosis in GV oocytes**

373 (A) Schematic of overexpressing *Chk1* WT and R442Q in mouse zygotes by mRNA
374 microinjection (Created with BioRender.com).

375 (B) Bar plot showing Chk1 R442Q arrest the first cleavage. Ctrl, n=23. WT, n=48. R442Q,
376 n=51. All pooled from 2 separate experiments; one-way analysis of variance (ANOVA),
377 Bonferroni's test for individual comparisons. Bars are means ± s.e.m.

378 (C) Representative live cell images of zygotes microinjected with mRNA encoding Chk1 WT
379 and R442Q GFP fusion protein. White arrowheads point to the arrested embryos. Time is as
380 indicated. Scale bar, 100 μm.

381 (D) Schematics of overexpressing Chk1 WT and R442Q in mouse oocytes (Created with
382 BioRender.com). Microinjected GV oocytes were first blocked in the GV stage with
383 Cilostamide for 4h. GVBD rate and MII rate 4h, 12h, 16h after release from blocking were
384 counted.

385 (E) Bar plot showing Chk1 R442Q delay mouse oocytes development. Ctrl, n=50. WT, n=59.
386 R442Q, n=52. All pooled from 2 separate experiments. Bars are means ± s.e.m. Upper panel,
387 statistical analysis of the percentage of GVBD 4h after release, MII 12h, and 16h after release.
388 Two-way analysis of variance (ANOVA), Bonferroni's test for individual comparisons. Lower
389 panel, composite bar graph of percentages of GV, GVBD, and MII oocytes of Ctrl, Chk1 WT,
390 and R442Q groups.

391 (F) Representative live cell images of oocytes microinjected with mRNA encoding Chk1 WT
392 and R442Q GFP fusion proteins. Yellow and white stars point out GV arrested oocytes (4h),
393 and oocytes progressed to the MII stage (16h). Scale bar, 100 μm.

394

395

396 **Figure 3. A graded Chk1 activity differentially modulates DNA damage response and cell**
397 **cycle progression in the zygote**

398 (A) CHEK1 R442Q protein showed higher kinase enzyme activity compared to WT.
399 Luciferase based kinase assay normalized to WT group. 9 tests from 3 separate experiments.
400 Two-sided Student's t-test. Columns are means ± s.e.m.

401 (B) Dot plot quantification of γH2AX signal in arrested R442Q mouse zygotes compared to
402 control non-injected (Ctrl) and WT injected zygotes. Ctrl, n=66, WT, n=28. R442Q, n=58. All

403 pooled from 2 separate experiments. One-way analysis of variance (ANOVA), Bonferroni's
404 test for individual comparisons. Bars are means ± s.e.m.
405 (C) Representative γH2AX immunostaining images of Ctrl, Chk1 WT, and R442Q zygotes.
406 Yellow circles mark the paternal and maternal pronucleus. PB, polar body. Cyan, DAPI; pink,
407 γH2AX; gray, Chk1. Scale bar, 20 μm.
408 (D) γH2AX staining in CHEK1 inhibitor (0.1μM) rescued 2-cell embryos. Cyan, DAPI; pink,
409 γH2AX; gray, Chk1. Scale bar, 20 μm.
410 (E) Quantification of γH2AX signal in 0.1μM CHEK1 inhibitor-treated or non-treated WT and
411 R442Q 2-cell embryos. Chk1 WT embryos with or without inhibitor treatment, n=15 and 21.
412 Chk1 R442Q embryos with or without inhibitor treatment, n=8 and 20. One-way analysis of
413 variance (ANOVA), Bonferroni's test for individual comparisons. Bars are means ± s.e.m.
414 (F) 30 nM CHEK1 inhibitor treatment rescued the development of Chk1 R442Q zygotes. Chk1
415 WT embryos with or without 30nM inhibitor treatment, n=98 and 106. Chk1 R442Q embryos
416 with or without 30nM inhibitor treatment, n=106 and 101. All pooled from 4 separated
417 experiments. One-way analysis of variance (ANOVA), Bonferroni's test for individual
418 comparisons. Bars are means ± s.e.m.
419 (G) Representative images of Chk1 WT and R442Q injected embryos with or without 30 nM
420 inhibitor treatment at 48h post HCG. Scale bar, 100 μm.
421 (H) 30 nM CHEK1 inhibitor-treated embryos can develop to the blastocyst stage. Chk1 WT,
422 n=48. Chk1 R442Q, n=46. All pooled from 2 separate experiments. Two-way analysis of
423 variance (ANOVA), Bonferroni's test for individual comparisons. Bars are means ± s.e.m.
424 (I) Representative images of 8-cell and blastocysts developed from zygotes injected with
425 mRNA of Chk1 WT and R442Q then treated with 30 nM CHEK1 inhibitor. The stage is as
426 indicated. Scale bar, 100 μm.
427 (J) Immunostaining of Oct4 and Nanog in blastocysts developed from WT or R442Q zygotes
428 treated with 30 nM CHEK1 inhibitor. The dashed line highlights the ICM region. Blue, DAPI;
429 green, Oct4; pink, Nanog. Scale bar, 20 μm. ICM, inner cell mass.
430 (K) Statistic analysis of total cell number, the ratio of Oct4, and Nanog positive cells in
431 blastocysts derived from Chk1 WT and R442Q injected zygotes with or without inhibitor
432 treatment. WT embryos with or without 30nM inhibitor treatment, n=19 and 15. R442Q
433 embryos with or without 30 nM inhibitor treatment, n=17 and 13. All pooled from 2 separate
434 experiments. One-way analysis of variance (ANOVA), Bonferroni's test for individual
435 comparisons. Bars are means ± s.e.m.

436

437 **Figure 4. A low dosage of CHEK1 inhibitor treatment does not affect zygotic genome**
438 **activation and permitted normal embryo development**

439 (A) Schematic of Chk1 WT and R442Q embryos used for RNA-Seq analysis (Created with
440 BioRender.com). Chk1 WT or R442Q mRNA were injected into mouse zygotes. One-cell
441 embryos were harvested at 6h (WT) or 10h (R442Q) post-injection. Two-cell embryos were
442 collected 30h post-injection. For blastocysts, Chk1 WT and R442Q injected zygotes were first
443 treated with 30nM inhibitor overnight. After washing off the inhibitor, 2-cell embryos were
444 cultured to the blastocyst stage and used for RNA-seq.

445 (B) PCA analysis of RNA-Seq data from single WT and R442Q embryos.

446 (C) Heatmap clustering of WT and R442Q zygotes and 2-cell stage embryos.

447 (D) Schematic of Chk1 WT and R442Q injected zygotes with or without 30 nM of CHEK1
448 inhibitor treatment, followed by transferring to pseudopregnant female mice (Created with
449 BioRender.com).

450 (E) Chk1 WT and R442Q embryos treated with or without 30 nM of inhibitor developed to
451 live pups with normal body weight after transplantation. n=15, 8, 17, and 14 live pups of Chk1
452 WT, R442Q, WT with inhibitor, and R442Q with inhibitor group. All pooled from 2 separate
453 experiments.

454

455 **Supplemental figure 1. *CHEK1* gene locus and *CHEK1* R442Q expression in somatic cells**
456 **of carriers**

457 (A) Human *CHEK1* gene locus and amino acid sequence of CHEK1 protein C-terminus. The
458 R442 in human CHEK1 protein is conserved among all species.

459 (B) No *CHEK1* R442Q mutation was detected by Sanger sequencing in patients' father's
460 siblings. Single peak of G read indicates the normal *CHEK1* allele.

461 (C) *CHEK1* is expressed in somatic cells of carriers verified by RT-PCR and agarose gel
462 electrophoresis.

463 (D) Detection of the ratio of *CHEK1* R442Q mutant RNA transcript by Sanger sequencing. 10
464 colonies were picked and sequenced for each sample.

465

466 **Supplemental figure 2. Chk1 localization in mouse oocytes and preimplantation embryos**

467 (A) Chk1 protein localizes to both nuclear and cytoplasm in mouse early embryos. Red, Chk1;
468 blue, DAPI. Scale bar, 20 μm.

469 (B) Microinjection of mRNA encoding Chk1 WT and R442Q GFP fusion protein leads to an
470 elevation of Chk1 and GFP protein expression in zygotes and 2-cell embryos. Ctrl, n=10. WT,
471 n=34. R442Q, n=33. All pooled from 2 separate experiments. One-way analysis of variance
472 (ANOVA), Bonferroni's test for individual comparisons. Bars are means ± s.e.m.
473 (C) Chk1 protein locates in the germinal vesicle and on the spindle of mouse oocytes. Red,
474 Chk1; blue, DAPI; green, Tubulin. Scale bar, 20 μm.
475 (D) Microinjection of mRNA encoding Chk1 WT and R442Q GFP fusion protein into GV
476 oocytes leads to an elevation of Chk1 and GFP protein expression. Ctrl, n=38. WT, n=39.
477 R442Q, n=44. All pooled from 2 independent experiments. One-way analysis of variance
478 (ANOVA), Bonferroni's test for individual comparisons. Bars are means ± s.e.m.
479
480 **Supplemental figure 3. CHEK1 R442Q showed an elevated kinase activity compared to**
481 **WT.**
482 (A) Schematic of human CHEK1 protein domains.
483 (B) Coomassie blue staining showing purification of CHEK1 N-term, WT, and R442Q proteins.
484 M, marker. Arrow points to the purified His-tagged proteins.
485 (C) Western blot showing His-tag purified CHEK1 N-term, WT, and R442Q proteins.
486 (D) Kinase assay showed CHEK1 R442Q mutant protein had increased kinase activity
487 compared to WT protein. n=9 from 3 independent experiments. Two-sided Student's t-test.
488 Columns are means ± s.e.m.
489
490 **Supplemental figure 4. A high concentration of CHEK1 inhibitor treatment caused DNA**
491 **damage**
492 (A) Quantification of Chk1 and GFP protein levels in zygotes injected with mRNA encoding
493 Chk1 WT and R442Q GFP fusion proteins. Related to Figure 3C. n=66 Ctrl zygotes, n=28 WT
494 oocytes, and n=58 R442Q oocytes, pooled from 2 separate experiments. One-way analysis of
495 variance (ANOVA), Bonferroni's test for individual comparisons. Bars are means ± s.e.m.
496 (B) High concentration of CHEK1 inhibitor (>100 nM) rescue the Chk1 R442Q injected
497 embryos to the 2-cell stage at 48h post HCG. Chk1 WT injected embryos with or without
498 inhibitor treatment, n=41 and 29; Chk1 R442Q injected embryos with or without inhibitor
499 treatment, n=44 and 24. All pooled from 2 separate experiments. One-way analysis of variance
500 (ANOVA), Bonferroni's test for individual comparisons. Bars are means ± s.e.m.
501 (C) High concentration of CHEK1 inhibitor (500 nM) leads to increased DNA damage
502 response in WT and R442Q 2-cell embryos. Blue, DAPI; purple, γH2AX. Scale bar, 20 μm.

503 (D) CHEK1 inhibitor concentration lower than 100 nM did not increase DNA damage response
504 in mouse early embryos. n=15,13,21,22,15 and 23 of Ctrl, 10 nM, 50 nM, 100 nM, 300 nM
505 and 400 nM inhibitor-treated groups. One-way analysis of variance (ANOVA), Bonferroni 's
506 test for individual comparisons. Bars are means ± s.e.m.
507 (E) Representative images of mouse embryos treated with different concentrations of CHEK1
508 inhibitor 48h post HCG from (D). Blue, DAPI; gray, γH2AX. Scale bar, 20 μm.
509 (F) Comparing Chk1 and GFP protein levels in 2-cell embryos injected with mRNA encoding
510 Chk1 WT and R442Q GFP fusion protein at PN3 zygote stage and treated with or without 0.1
511 μM of CHEK1 inhibitor, related to Figure 3D. WT embryos with or without inhibitor treatment,
512 n=15 and 21. R442Q embryos with or without inhibitor treatment, n=8 and 20. All pooled from
513 2 separate experiments. One-way analysis of variance (ANOVA), Bonferroni's test for
514 individual comparisons. Bars are means ± s.e.m.
515 (G) Chk1 WT and R442Q mouse embryos treated with 30 nM of inhibitor developed to live
516 pups with normal body weight after transplantation. Related to Figure 4E.
517
518 **Supplementary figure 5. Transcriptome analysis of mouse embryos injected with mRNA**
519 **of Chk1 WT and R442Q**
520 (A) Volcano plot depicting significantly differentially expressed genes in zygotes and 2-cell
521 embryos injected with mRNA of Chk1 WT (n=5 zygotes, n=4 2-cell embryos) and R442Q
522 (n=6 zygotes, n=5 2-cell embryos).
523 (B) Bubble plots showing the major GO terms of differentially expressed genes enriched in
524 Chk1 WT and R442Q zygotes and late 2-cell embryos.
525
526

Figure 1. First mitosis failure in zygotes from *CHEK1* R442Q females

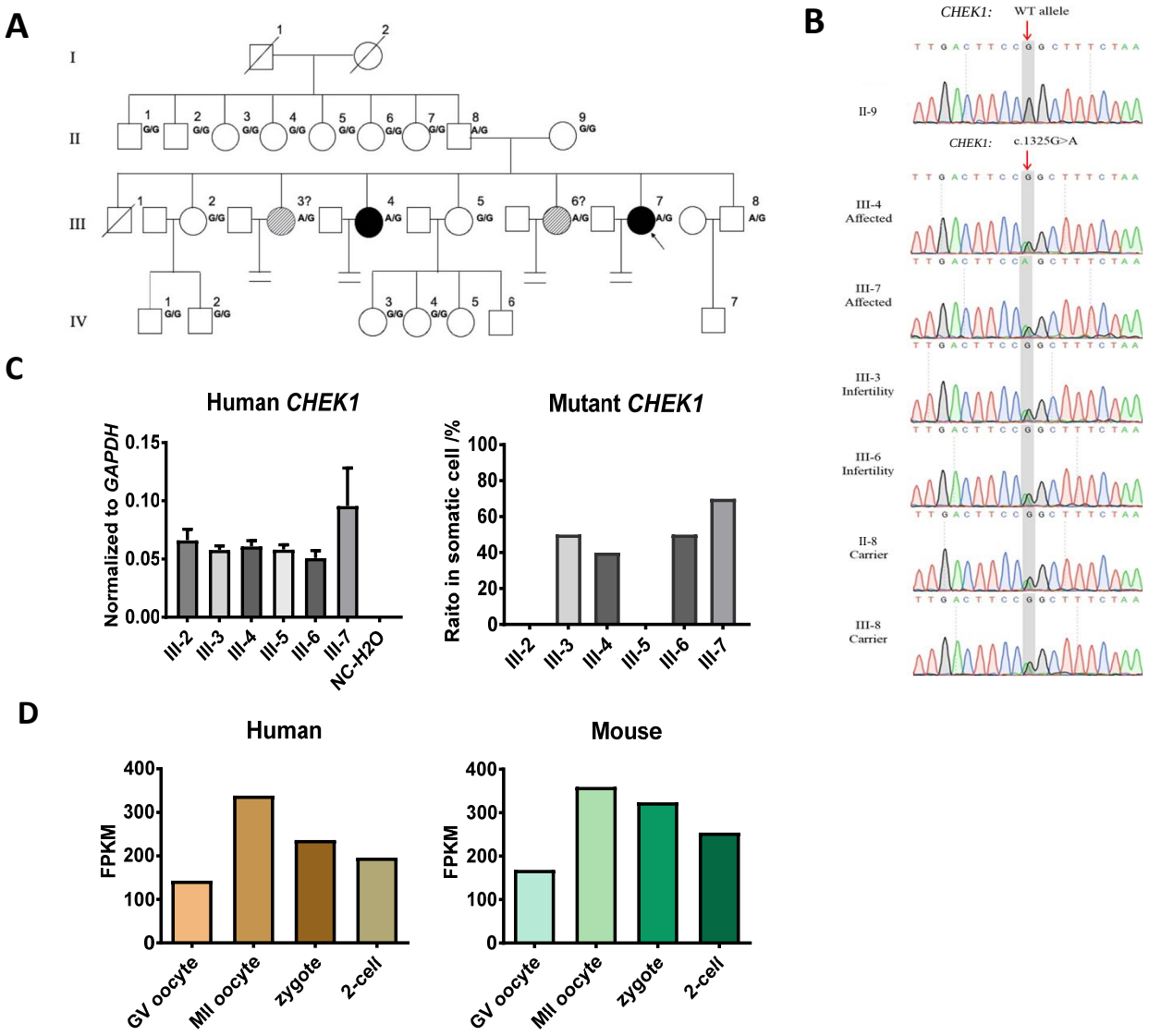

Figure 2. Overexpression of *Chk1* R442Q inhibited the first mitosis in mouse zygotes and meiosis in GV oocytes

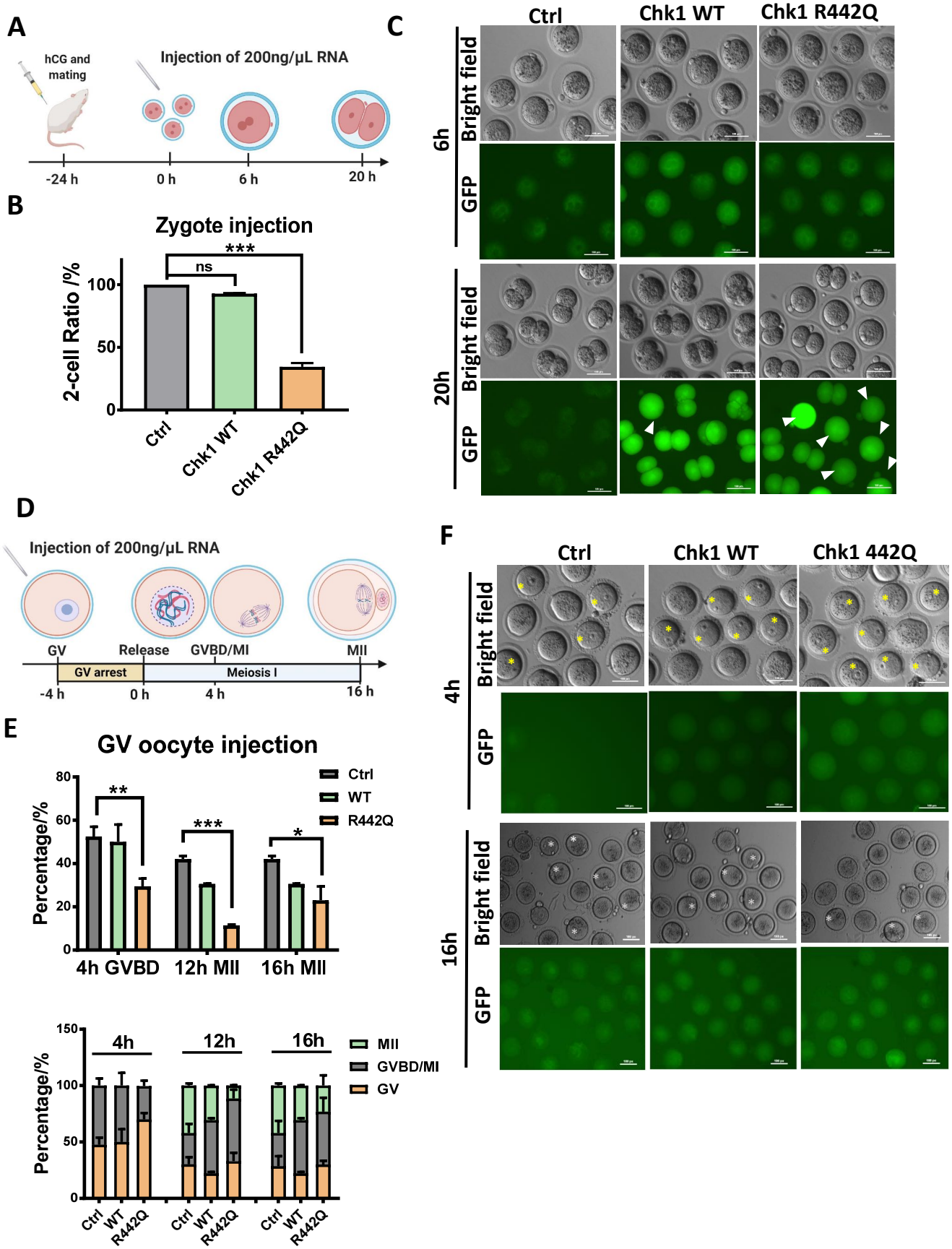

Figure 3. A graded Chk1 activity differentially modulates DNA damage response and cell cycle progression in the zygote

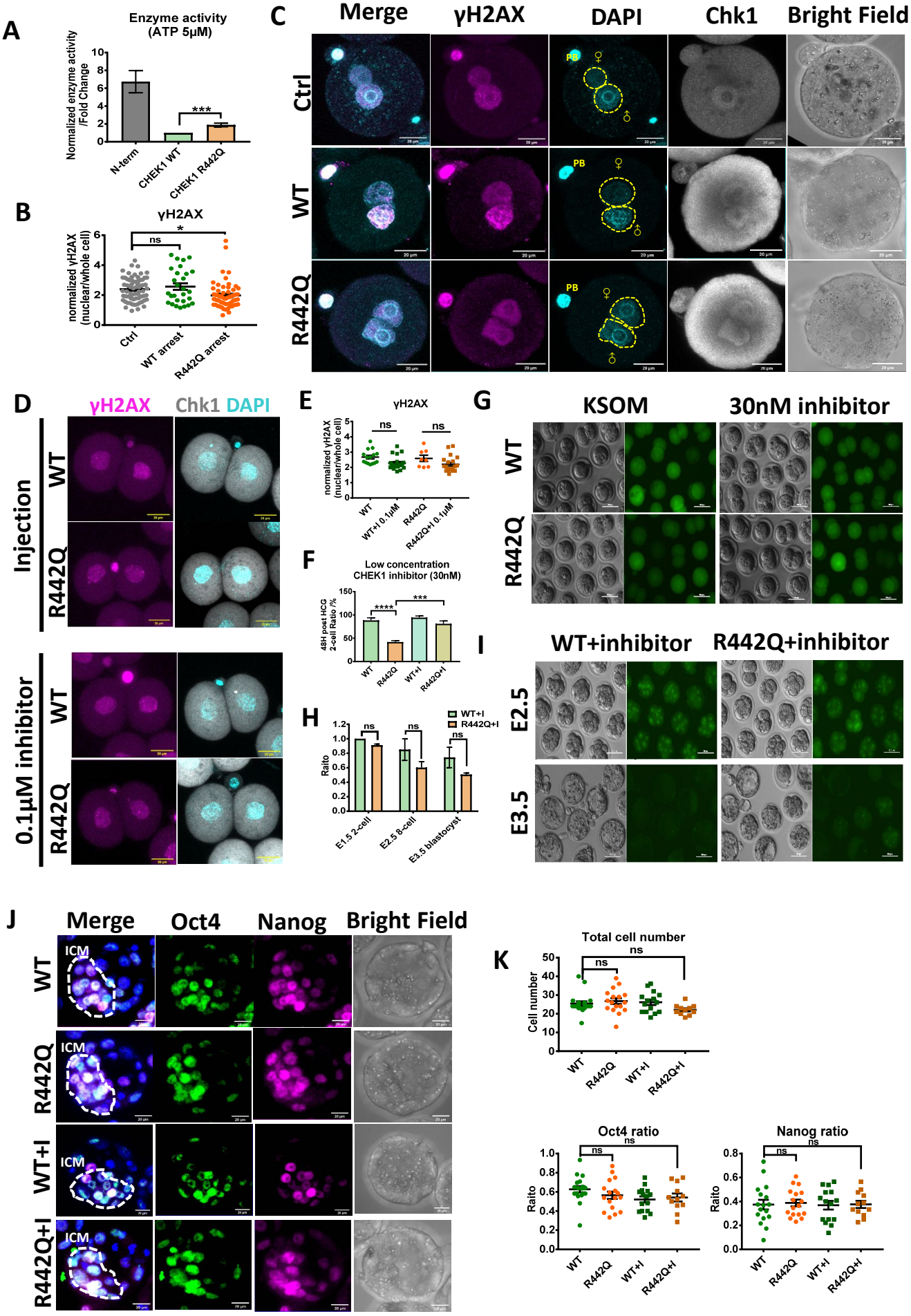

Figure 4. A low dosage of CHEK1 inhibitor treatment does not affect zygotic genome activation and permitted normal embryo development

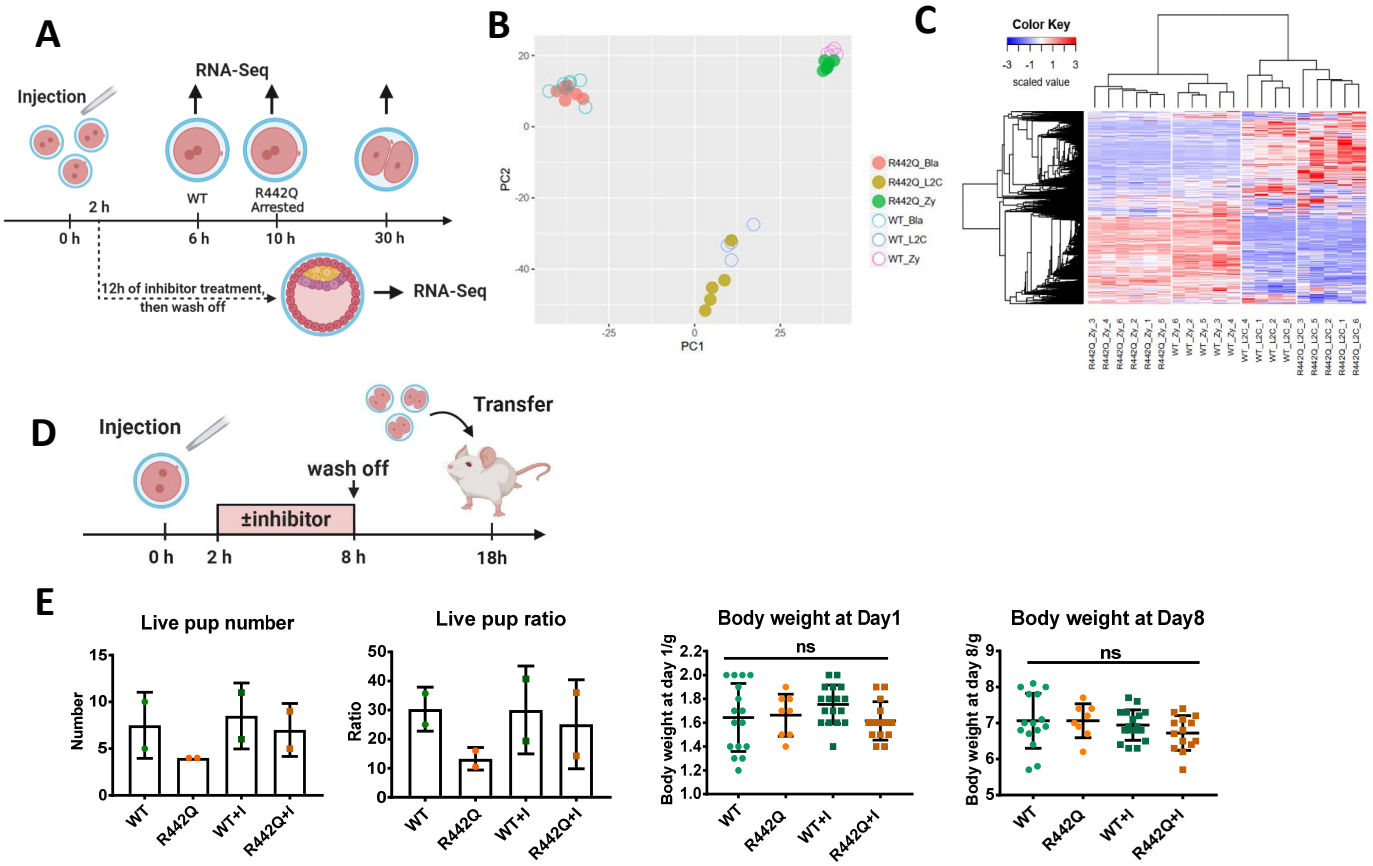

Supplemental figure 1. CHEK1 gene locus and CHEK1 R442Q expression in somatic cells of carriers

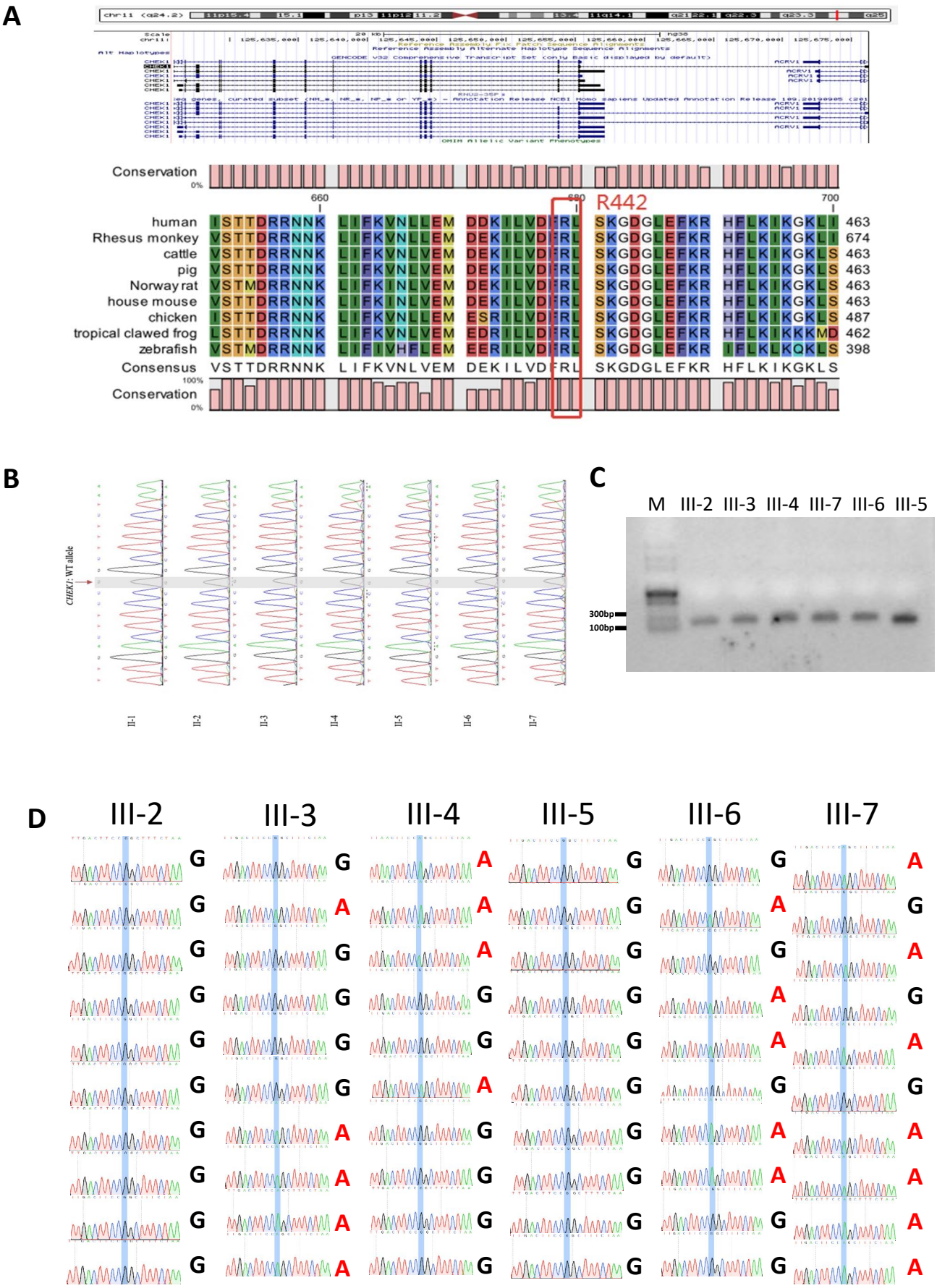

Supplemental figure 2. Chk1 localization in mouse oocytes and preimplantation embryos

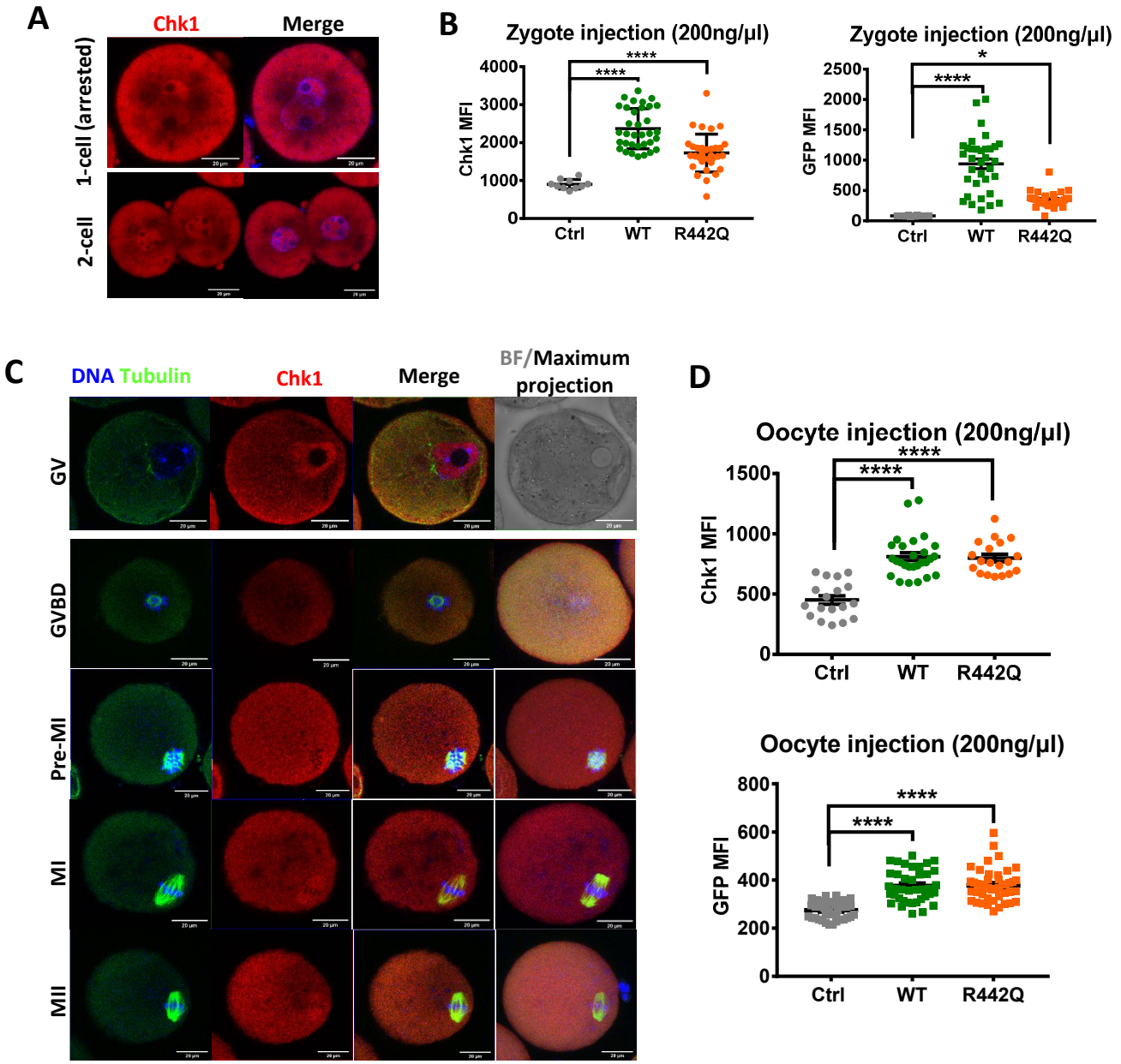

Supplemental figure 3. CHEK1 R442Q showed an elevated kinase activity compared to WT

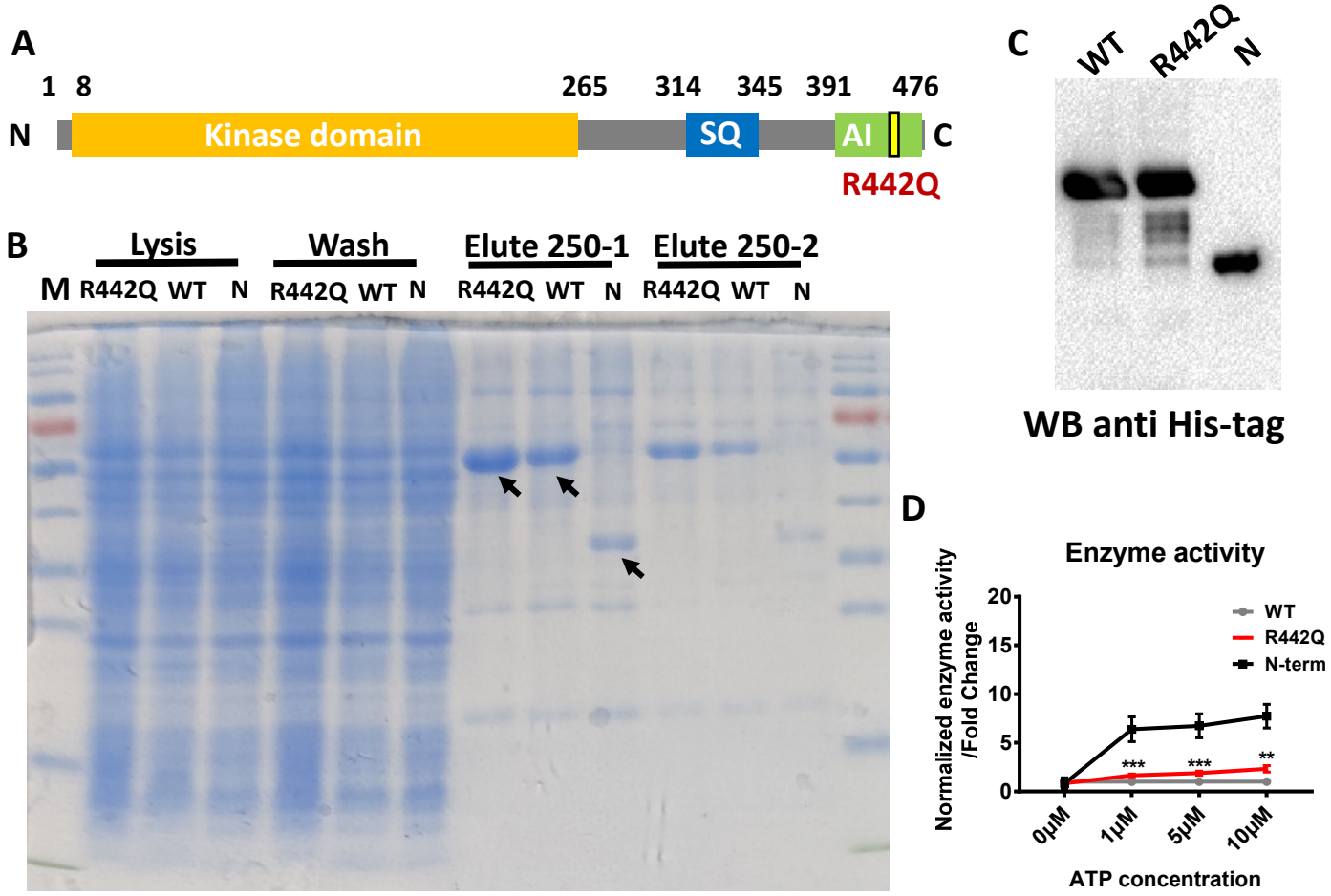

Supplemental figure 4. A high concentration of CHEK1 inhibitor treatment caused DNA damage

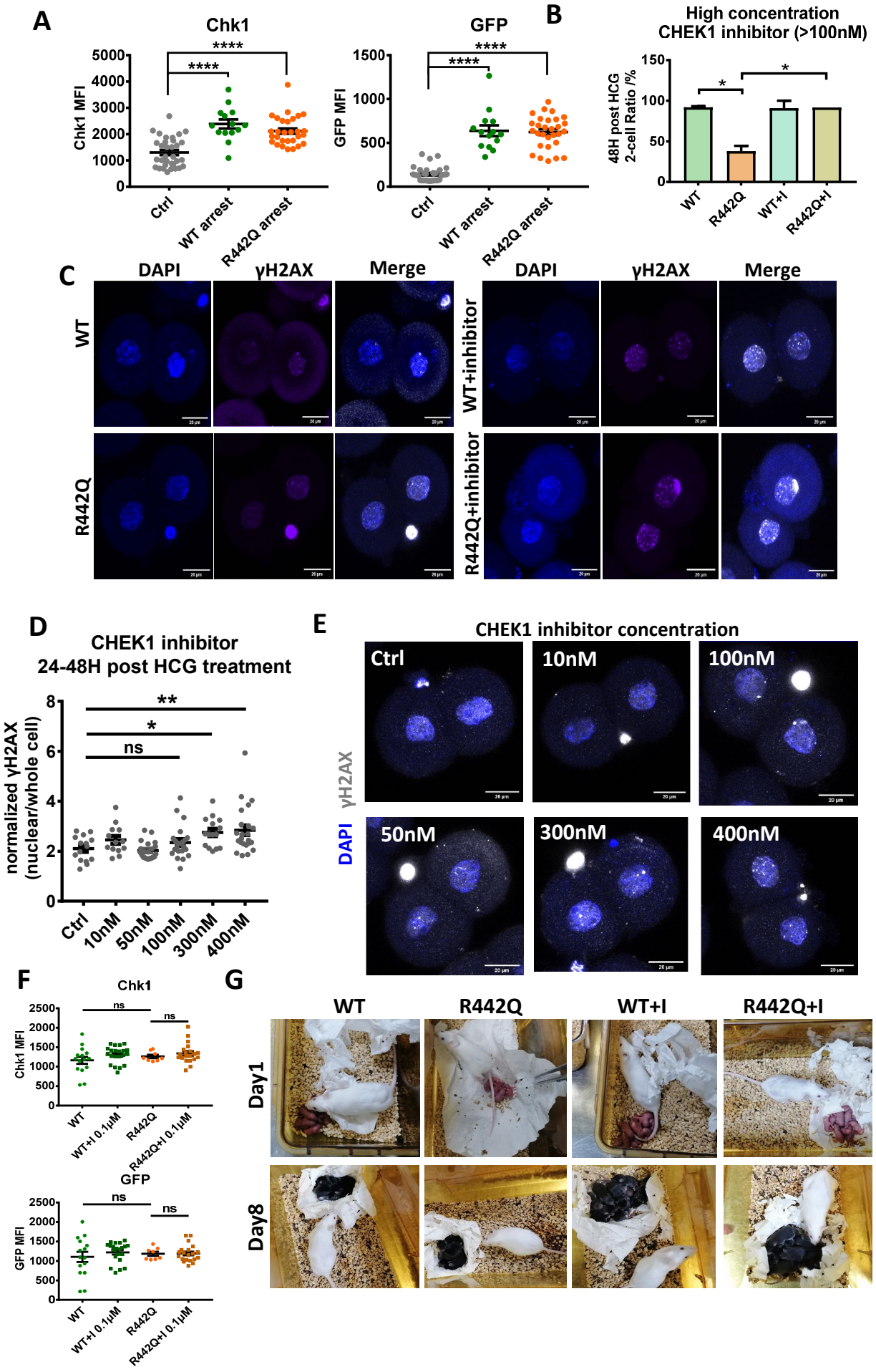
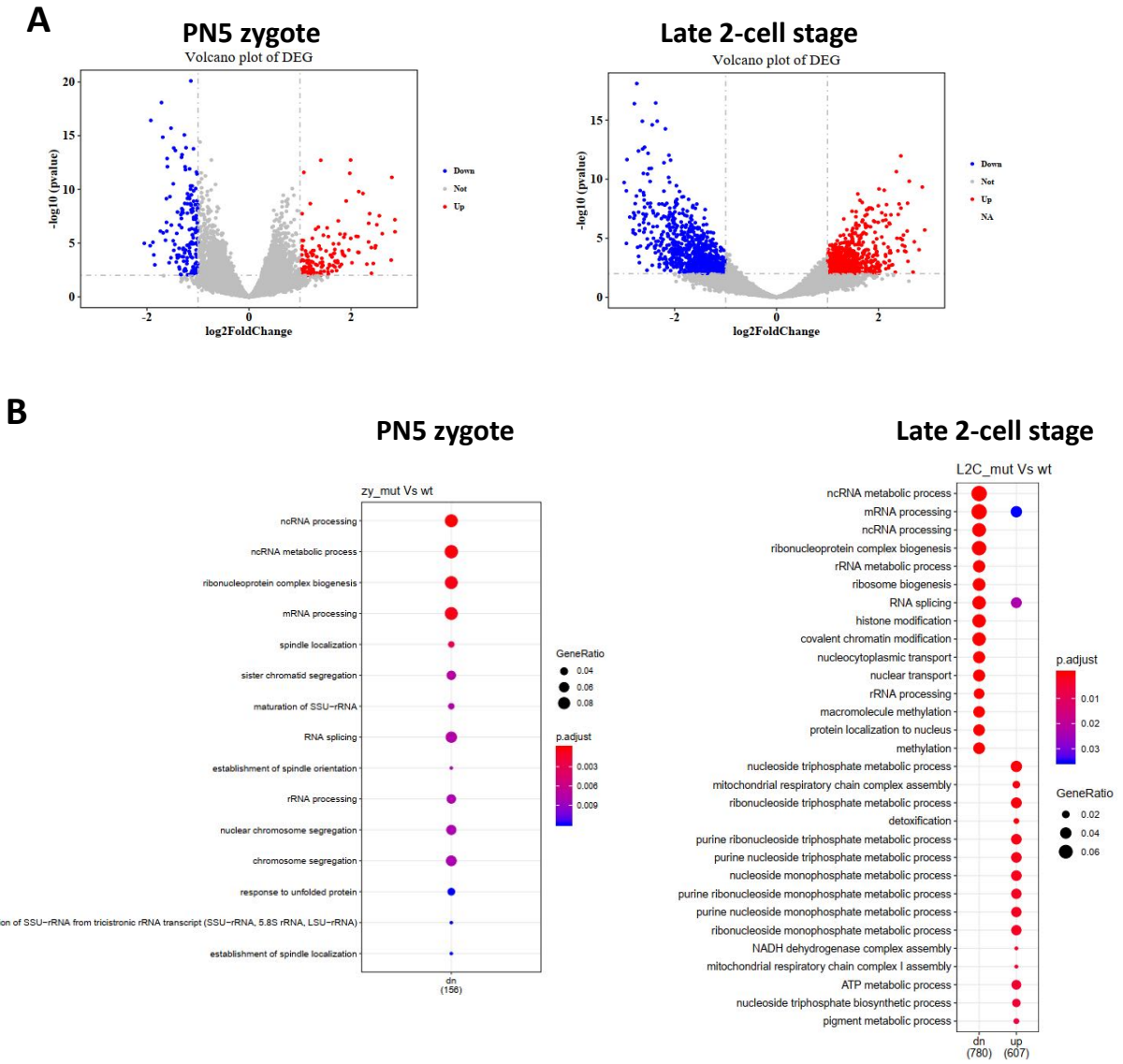
Supplementary figure 5. Transcriptome analysis of mouse embryos injected with mRNA of Chk1 WT and R442Q